Petroleum & Coal
ISSN 1337-7027

Available online at www.vurup.sk/petroleum-coal
Petroleum & Coal 56(5) 532-543, 2014

SEISMIC ATTRIBUTE UTILIZATION FOR STRUCTURAL PATTERN DETECTION, FAULT IMAGING AND PROSPECT IDENTIFICATION

Oluwatosin John Rotimi[1,2*], Zhenli Wang[2], Bankole D. Ako[3] and C. C. Uhuegbu[4]

[1]*Petroleum Engineering Department, Covenant University, Ota, Nigeria;* [2]*Institute of Geology and Geophysics, Chinese Academy of Science, Beijing, China ;*[3]*Department of Applied Geophysics Federal University of Technology (FUTA), Akure, Ondo State, Nigeria,*
[4]*Department of Physical and Geosciences, Godfrey Okoye University, Enugu state, Nigeria*
[*]Corresponding author: tossynrotimmy@yahoo.com, oluwatosin.rotimi@covenantuniversity.edu.ng

Received July 16, 2014, Accepted November 5, 2014

Abstract

Structural pattern mapping and modeling for structural styles delineation and prospect identification in the complex Xinglongtai-Majuanzi structure, Liaohe depression, China is a concern in exploring for hydrocarbon. This is as a result of the occurrence of varied faulting pattern and sub-seismic faults. Analysis was on attributes computed from migrated 3D seismic data, with support from well logs from the area. Architectural assessment, structural delineation and prospect analysis was done on the portion of the massive sag structure proven to have originated in the Paleogene period. Combinations of structural and stratigraphic attributes were used in evaluating the nature of the fairly consolidated turbidite deposits of the hydrocarbon prolific Shahejie formation amidst numerous syndepositional faults. Results indicate that normal and reverse faults are quite common in the study area with dipping angle between 50 and 80 degrees. The deposits of interbeded sand shale sequences are characterized by non-uniformity in strata arrangement. The stratigraphy of the area is observed as dipping sub-parallel and chaotic clinoforms which terminates in a thick wedge structure in the distal portion. This pattern is bestowed by the interplay of both the underlying regional and overlying sub-regional strike slip faults. This has increased the heterogeneity of the petrophysical parameters observed for the facies models and thereby assisted in understanding structural trapping configuration for the play prospect of the area.

Keywords: attributes; structural styles; stratigraphy; characterization; prospects; facies.

1. Introduction

The structural pattern of the western sag in the Xinglongtai-Majuanxi structure (figures 1 and 2) is a complex one that originates from the major regional structural pattern in the area. The basin being an inland basin (intracratonic) has evolved by strike-slip tectonics; consequently this has in turn to varying degrees impacted on the attitude of the overlying formations. This rift basin of the Cenozoic has evolved through two important stages of rifting in the Paleocene and a depression stage in the Neogene, thereby accounting for the thick Cenozoic strata that include the Shahejie formations (1,2,3) encountered in the study field [10]. The Xinglongtai-Majuanxi structure studied has series of fault echelon and comb structures. These syndepositional structures are prevalent and characterize the rift subsidence nature of the terrain.

This compressional slump structural pattern has a close semblance with the growth faulting patterns characteristic of the wave dominated deltaic petroleum system [6-7], but in this case no roll-over anticlines are associated with the faults. Also, the normal listric fault have collapsed crest and hence form drapes on the adjacent units. In some cases this initiates the formation of adjoining thick pile of sediments (figure 3). This is believed to be responsible for the complex bedforms and formations characterized by gradual lateral changes in lithofacies with abrupt boundaries horizontally and in different depositional facies. This is the common pattern in the Xinglongtai-Majuanzi structure where unique faulting orientations are in different seismic

facies (figure 3). Prevailing fault orientation is northeast/southwest, dipping south-easterly and trending northwest-southeast direction. This is in response to the alternating compressional and extensional forces from the underlying Shuangxi hidden strike-slip fault in the volcanic basement rock of the eastern sag and the overriding major Tanlu fault that traverses the Liaohe western sag [10-12]. Hong [3] documented Taian Dawa fault as the controlling fault of the Liaohe western sag, and as the western of the two sub-faults of the Tanlu fault in the Liaohe Depression [10].

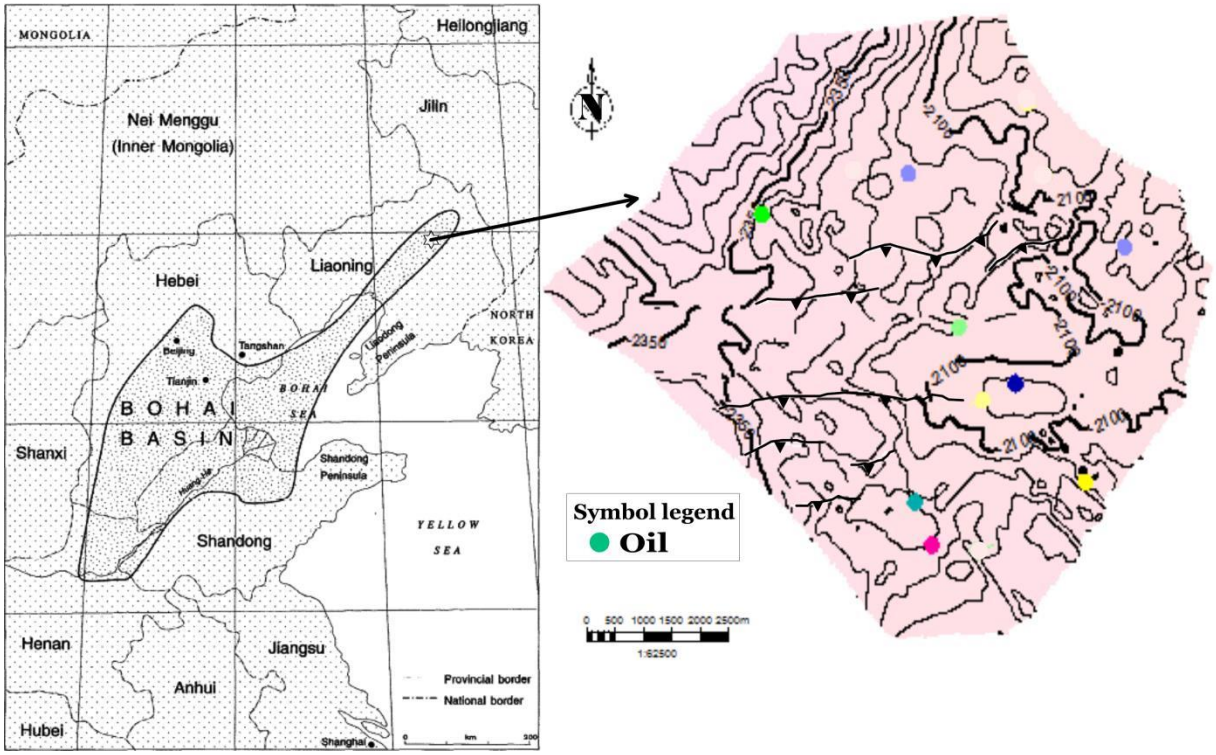

Figure 1 Location of the Xinglongtai-Majuanxi with depth structure map for the study area and the available wells within the survey

The objective of this study is to re-evaluate the likelihood of production induced structural pattern in this portion of Liaohe depression. This is after some episode of hydrocarbon production. It is targeted at making decisive secondary recovery method suitable for draining the remaining prospect. The principles of structural analysis via seismic attributes and stochastic simulations are utilized.

2. Materials and methods

The workflow utilized migrated depth converted 3D seismic data and well logs. Check-shot velocity data and sonic was used in converting the seismic data to depth (Figure 3). Seismic attributes were computed in the vicinity of tracked horizons using the seismic volume attribute library in Petrel software. The analysis started with the application of structural attributes that makes discontinuity and pattern dip clearer in seismic reflection events (Figure 4). Understanding pattern was best achieved by visualizing seismic lines opened in the strike direction (inline). For this dataset, a total of 780 lines were available. 78 lines were interpreted for stratigraphic and structural delineations. To enable clearer representation of both stratigraphic and structural elements, a total of 260 lines were used. A jump step of 10 each was used on the total 360 inlines and 420 crosslines for interpretation. For most structural attribute computation such as Gaussian spatial smoothing with emphasis on enhanced edge and dip guide, sample trace of 3 was used in both strike and dip direction. In the vertical direction, 15 milliseconds range was adopted as a maximum window for attribute computation (Figure 5).

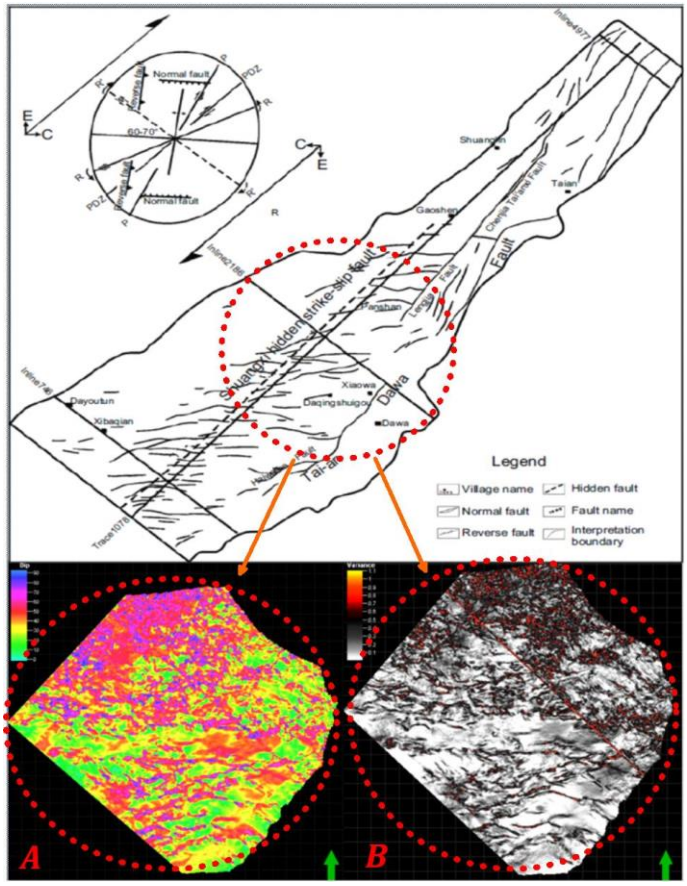

Figure 2 Regional structural pattern of study area showing major strike-slip faults. A and B are results of geometric attribute enhanced structural attitude. Same location captured in red ovals

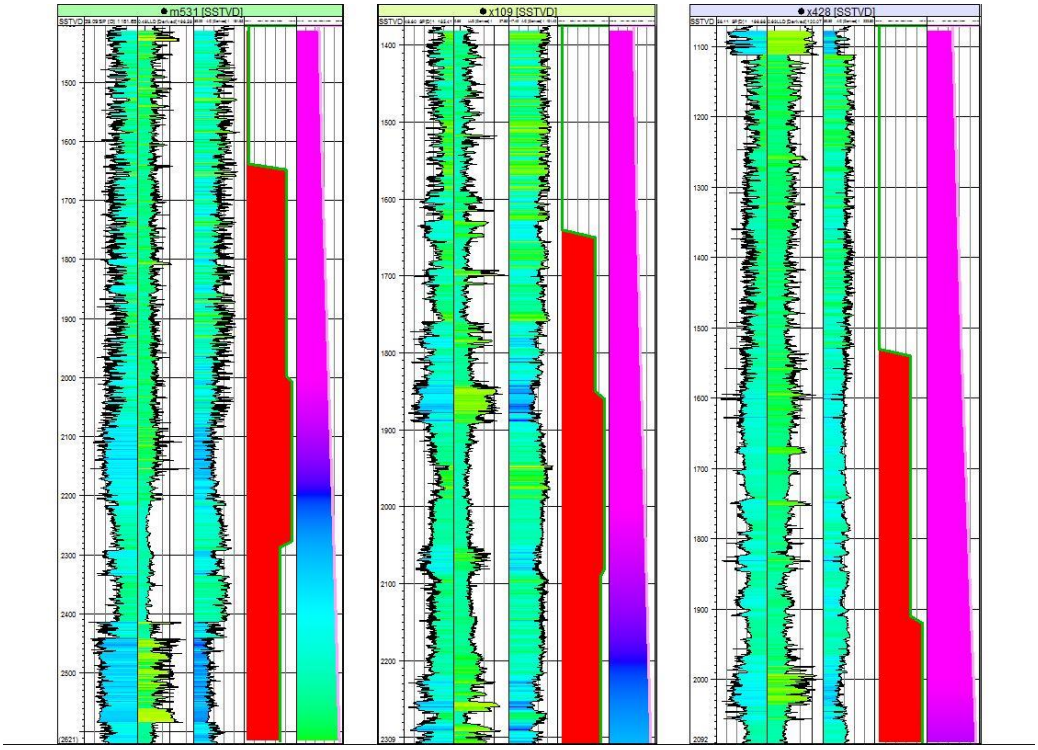

Figure 3 Well log panel showing 3 of the logs used. 5 tracks presented has SP log, resistivity log, Acoustic log, Velocity model and One way Travel time respectively

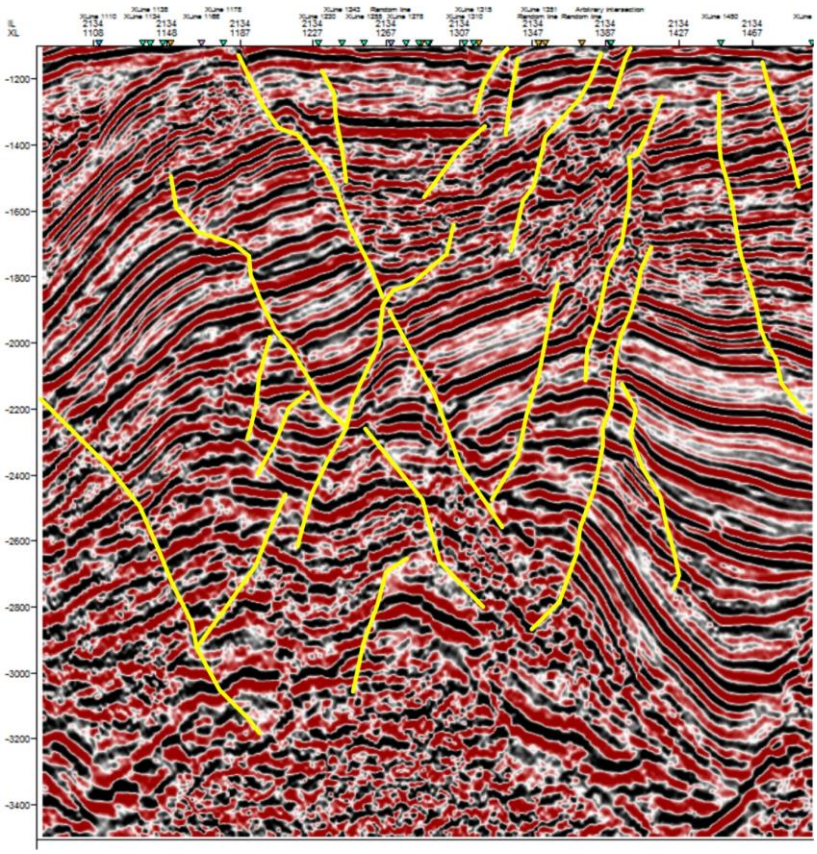

Figure 4 Seismic inline 2134 with different faulting orientation per facies

Amplitude constrained quadrature trace assisted in observing the velocity difference typified by trace polarity and preserved in amplitude strength of the seismic data. Time slices on this attribute gave a clearer texture feature of lithological discontinuities for accurate mapping of faults. Cosine of phase attribute was also computed. This assisted in identifying continuity and termination of reflection events in stratigraphic interpretations [1-2, 4, 8-9, 11]. Other seismic attributes used are Coherency, Principal component analysis (PCA) constrained to local structural dip, root mean square (rms) amplitude, instantaneous amplitude.

3. Results and discussion

3.1 Structural imprints

Knowledge of the geology has been enhanced by the stratigraphic and structural characterization of the field using attribute oriented analytical approach. Basin evolution suggests a Tertiary to Recent age for the deposits [5]. This inference was from the clinoforms pattern on the seismic data analyzed. It is typified by a highly unconsolidated and chaotic interval amidst more parallel clinoforms indicating under-compaction and rapid deposition. This facies imprint belongs to the younger deposits of the alluvial fan depositional environment with high inclination as seen around inline 2050 and beyond. The evolutional history has confirmed that depositional style fluctuates in activity intensity, being weak at the beginning but amidst some cycles of rise and fall reach its strongest level in the late Oligocene [13].

Fault traces are clearer on the Variance (coherency) and PCA constrained to local structural dip of the interpreted seismic data displayed on inline 2070 and surface slice at approximately 1152 (Figure 5). Higher lateral coherency is observed on non-chaotic zones in the distal part with angle of dip changing spatially. These zones are characterized by high attribute values having anomalous coloration (red to yellow) on figure 5. Dipping beds are detected at those points with high values. They are points corresponding to locations of fault imprints and occurrence [8-9].

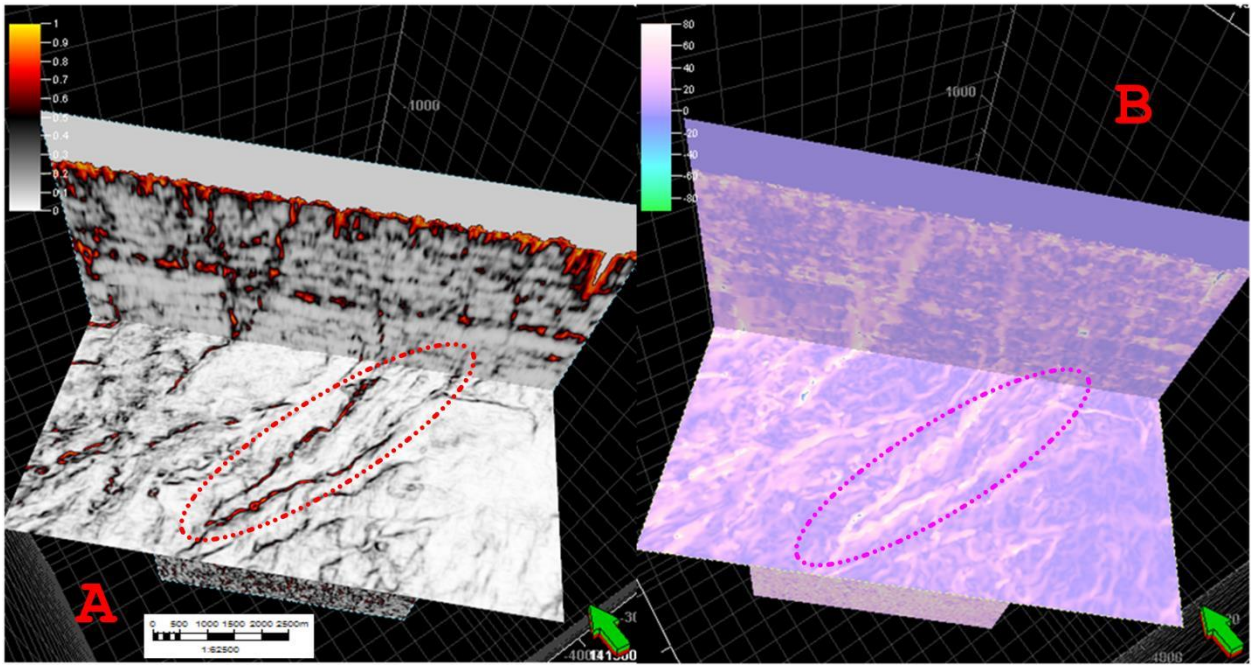

Figure 5 Variance cube on amplitude volume with enhanced edge effect (A) and amplitude volume PCA constrained to local structural dip (B) both shown on time slice and line 2070.

Computed volume of RMS amplitude and porosity predicted from multi attribute analysis assisted in delineating hydrocarbon prolific sand bodies within the zone. This step made easier conclusions about the packet of rock units that are hydrocarbon bearing amidst structural closures.

Outlined local portion and patches of shale lenses are observed as smeared infillings on seismic lines as seen on figure 6. This is an indication of compaction induced deformation with increase pressure at points having argillaceous minerals amidst clastic sediments. This is also an indication of potential seals occurrence on the flanks of the faults. The portion captured in ovals appears to be gas chimney zone but actually a zone of multiple sub-seismic micro-faults (Figure 6).

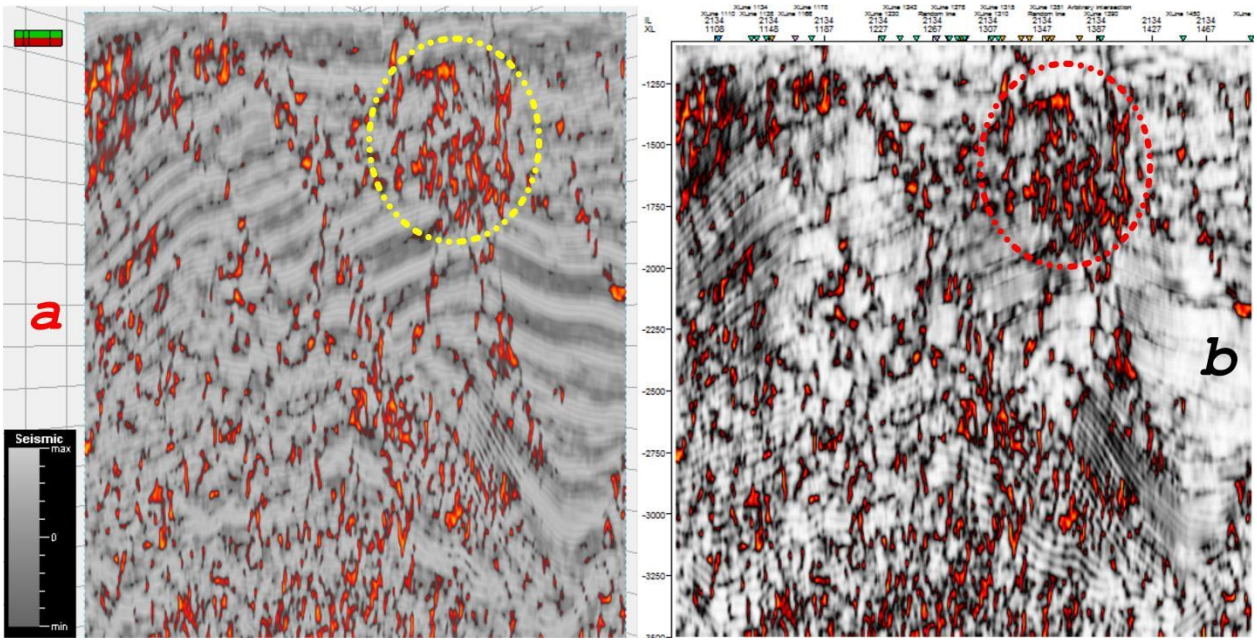

Figure 6 Filtered hot coherency component overlaying gray scale quadrature trace (a). Beside it is unfiltered continuity enhanced coherency volume (b) captured in ovals

Surface attribute maps (Figure 7 and 8) shows fault line patterns in different directions. Major faults runs in east-west direction with sand body within them, while minor faults captured in green ovals make 30 degrees to the major faults.

High variances have been observed to correspond with points of high structural dip, thus an indication of suitability in using principal component analysis constrained structural dip attribute computation in mapping structural architecture.

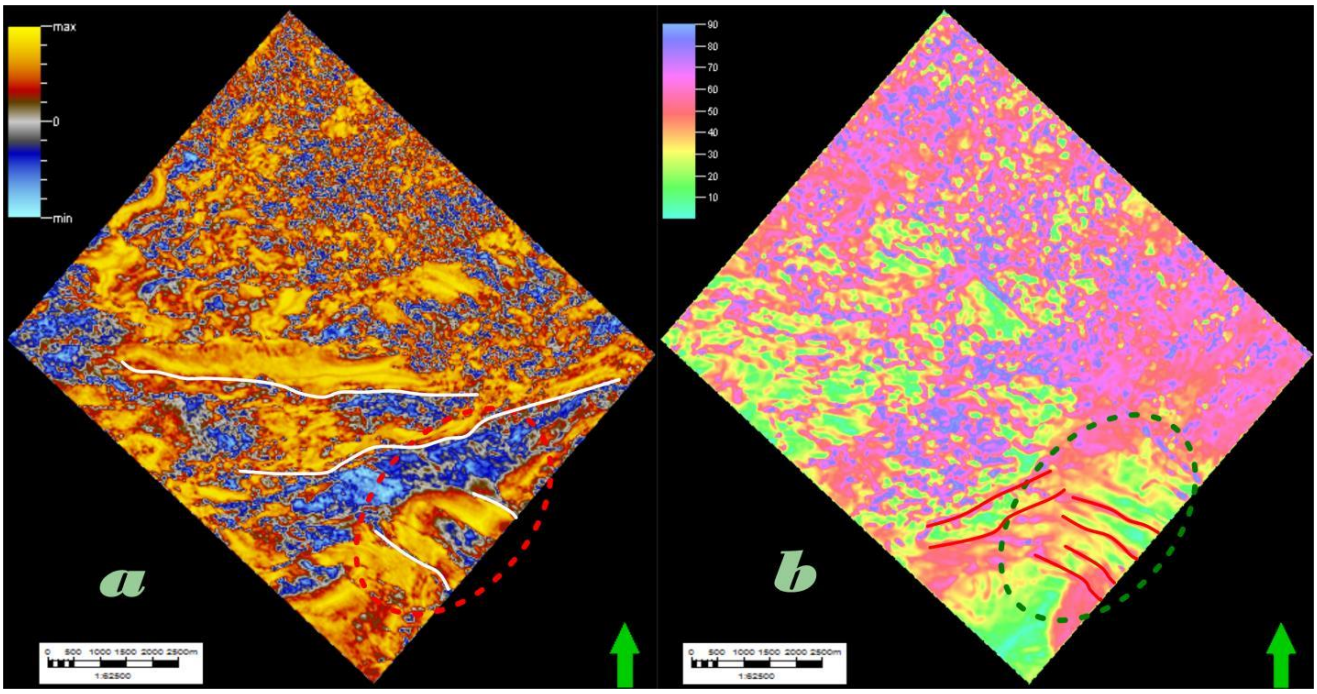

Figure 7 Surface attribute maps showing sand body fairways separated by subtle fault marked in white and red. a is rms amplitude covariance blend with enhanced edge effect. b is product of a and dip quadrature on red-green-blue scale

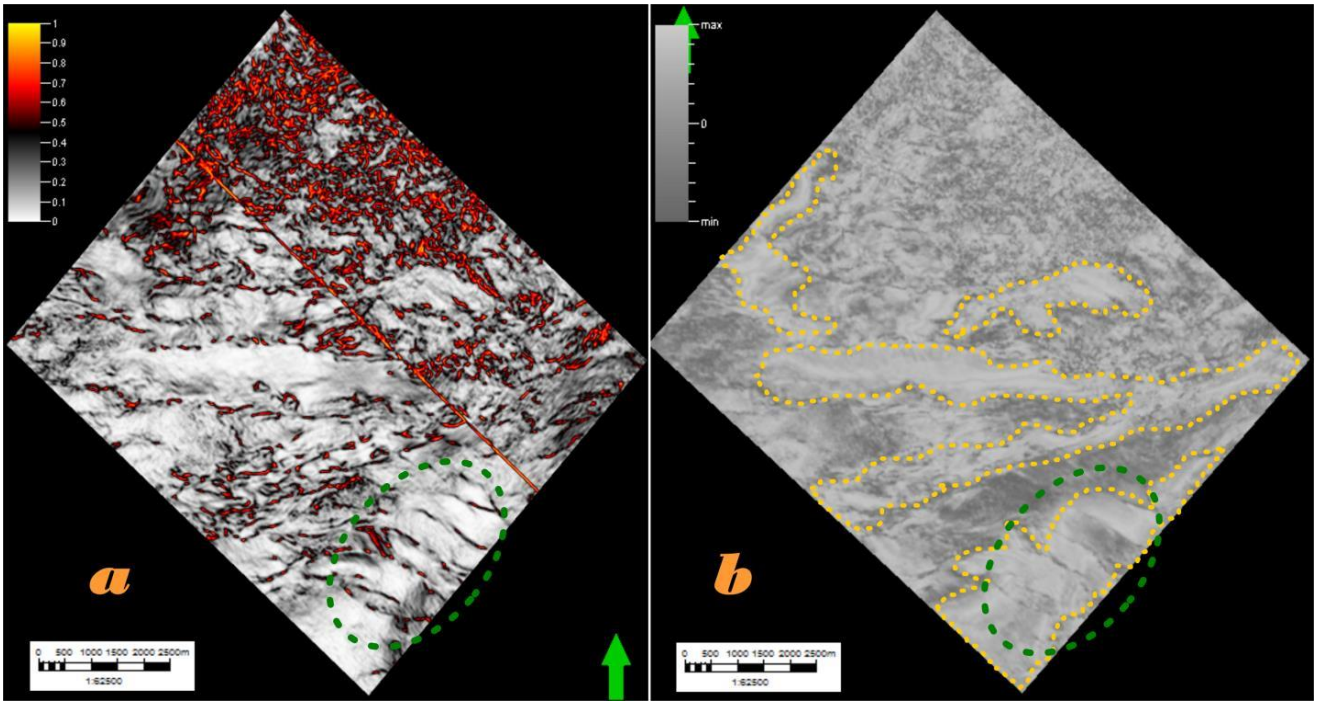

Figure 8 Surface attribute maps showing sand body fairways captured in gold broken lines. a is covariance blend with enhanced edge effect. b is product of a and rms amplitude on gray scale

3.2 Structural imprint on Static models

Static model of the total rock volume unit populated with lithofacies is characterized by both normal and reverse faults (Figures 9 and 10) with continuous lateral arrangement of lithological units on both sides of the fault. Generally, the dip of the major fault is between 60 and 80 degrees while the minor fault dips around 50 to 70 degrees (Figure 7 and 8). The heave varies from one fault to another but generally falls between 35 m and 50 m for thrust fault and between 70 m and 80 m on normal and reverse faults. The throw of the faults is between 20 m and 30 m on the thrust fault and between 20 m and 35 m on the normal and reverse faults.

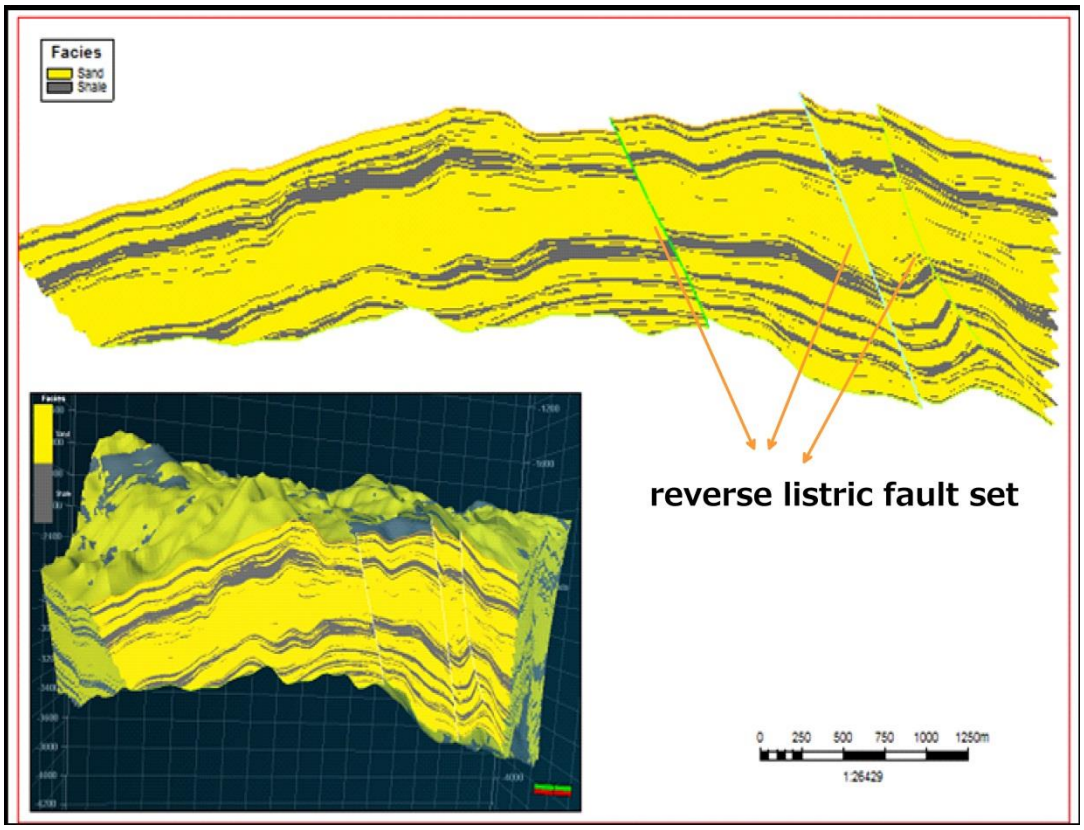

Figure 9 Zone model showing listric fault set

Occurrence and formation of structures studied is believed to be synsedimentary and partially production induced. This is probably borne out of the unstable and non-uniform fault pattern formed in response to the withdrawal of the supporting fluids in the faulted rock units as a result of post-depositional changes. Secondly, it may be a result of regional adjustment to the large scale structural pattern of the area. Since the rocks are fairly consolidated mixed sand-shale-grit units deposited within a wedge sag receptacle, adjustment of the receptacle walls makes for settlement and occurrence of varied structural imprints. Faults were activated in the northwest southeast portion and are trending in the southern direction. The average distance of the faults apart is between 700 m and to more than half the width of the modeled area (i.e. 6km, Figure 2, 4 and 9). In the distal portion, there is increased occurrence of thrust faults that are dipping with shorter distances in some location and some closing on the proximal earlier activated fault block. In figures 9-12, a sequence of fault reactivation is noticed as we move to the southern direction. Normal faults appear initially towards the middle of the zone while reverse faults appear beyond the normal fault separating the unit into blocks.

The earlier thrust faults are translational as they initially occur as vertical and then change to curved fault in response to dip in the distal portion. Occurrence of a combination reverse fault and normal fault activated a structurally uplifted block (horst block). Both the downthrown and up thrown faults blocks have lateral horizon continuity occurring in them. Here, the former hanging wall on the reverse fault becomes the foot wall on the latest listric normal fault with the third fault plane getting listric and dipping southerly (Figure 9). Other

features seen on this north-south intersection line for the zone are shown on Figure 10, as new set of fault reactivated in the distal portion in the alternate direction. A structurally depressed block (graben) appear after the sets of reverse fault at about 3.5km to the horst structure initially interpreted. This horst/graben reactivation keeps reoccurring further in the northern direction and the cycle continues with fault block maturity diminishing with the thickness of rock unit and in the dipping direction. Towards the middle of the model, the earlier fault planes observed disappear and new ones appear above it and other ones farther southerly.

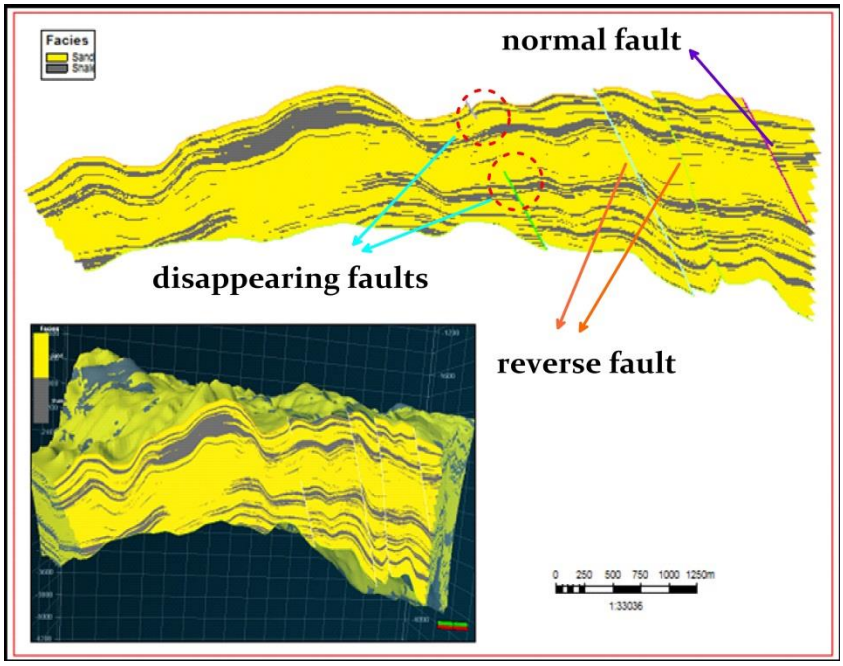

Figure 10 Zone model with fault types

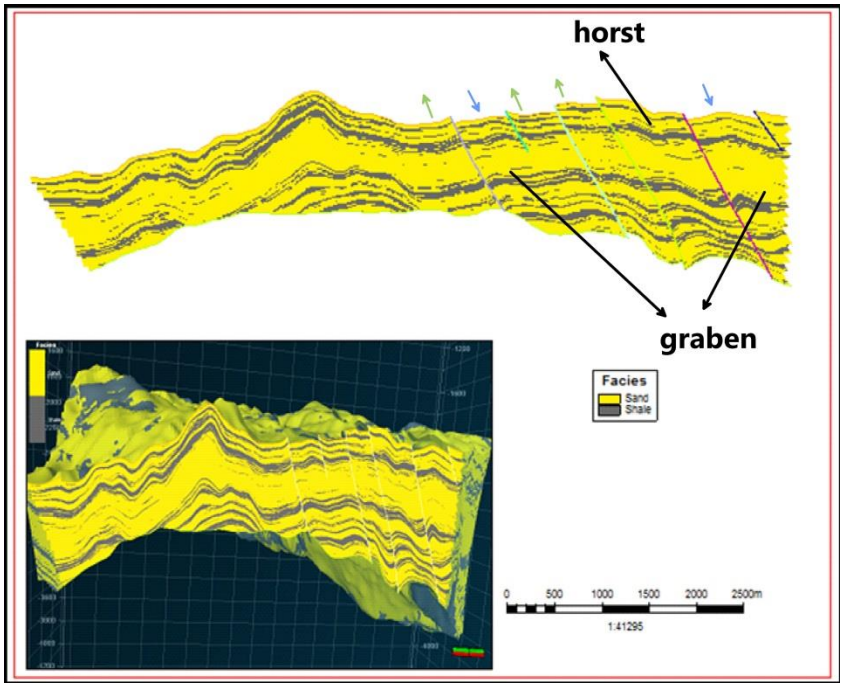

Figure 11 Zone model showing horst and graben features

Generally, newly activated southern fault is normal and in context the footwall block becomes a horst. Folding and rock rumpling is initiated at the lower portion of this zone. This is as a result of the increased exerted synsedimentary pressure prevalent in the southern direction

as progradation of sediments continues giving rise to the massive wedge structure in the dipping side of the study area. This southern part has dipping faults getting listric as they split stacked intercalations of sand and shale sequences. With distance and pressure variation (extensional and compressional forces in play and overburden influence), fault sets in echelon that appeared at some point begin to diminish in intensity and ability to cause discontinuity of the lateral expressions of the horizons (Figures 11 – 12).

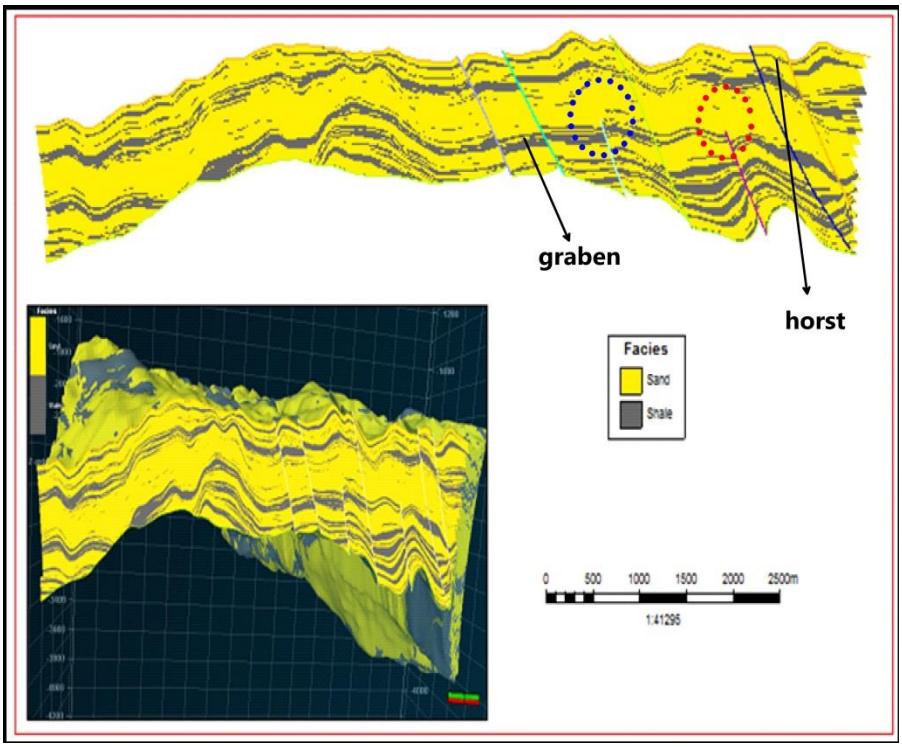

Figure 12 Zone model showing fault truncation/ disappearance giving rise to varied width of horst and graben

3.3 Stratigraphic configurations

Stratigraphic configurations observed are contemporaneous and linked to the basement topography. They are direct responses of synsedimentary structural patterns and features exhibited in the interpreted rock column. These developed from the interplay of factors such as accommodation (space for deposition), receptacle or basin structure, prevalent forces during deposition and pressure regimes (Figure 13). According to [10], "Liaohe western sag is a depressed structure unit, in the northeast of the Bohai bay basin and the western sub-fault" (Tanlu fault) traverses the sag. A central uplift portion separates the eastern sag adjacent to the western sag bordered by the Yanshan folding zones of the Jurassic-Cretaceous. Formation of structural sags is usually as a result of different tectonic activities and also the operation of synsedimentary and post-sedimentary forces (Figure 14). These forces are either compressional forces that gives rise to folded and thrust structures or extensional forces that produces dip-slip faults on rock bodies. Research has shown that on the regional scale, the strike-slip activities in the area have a unique start-up which began from the transition stage from uplift to depression. Two major strike slip episode are documented in the Liaohe basin named buried and interpretable [10]. The massive Shuangxi fault referred as the buried fault zone and the smaller interpretable strike-slip faults includes Hainan, Haiwahe, Tian Dawa, Lengjia, Chengjia -Tia'anxi and Niuxintuo faults [10] (Figures 2 and 4). The lower hidden Shuangxi fault is as a result of extensional activity in the Northwest-Southeast direction, whereas the assemblage of the fault system in the upper potion is interpreted by the dextral lateral strike-slip strain ellipse, meaning that the fault scheme of the upper strata formed under the control of regional dextral lateral strike-slip activity.

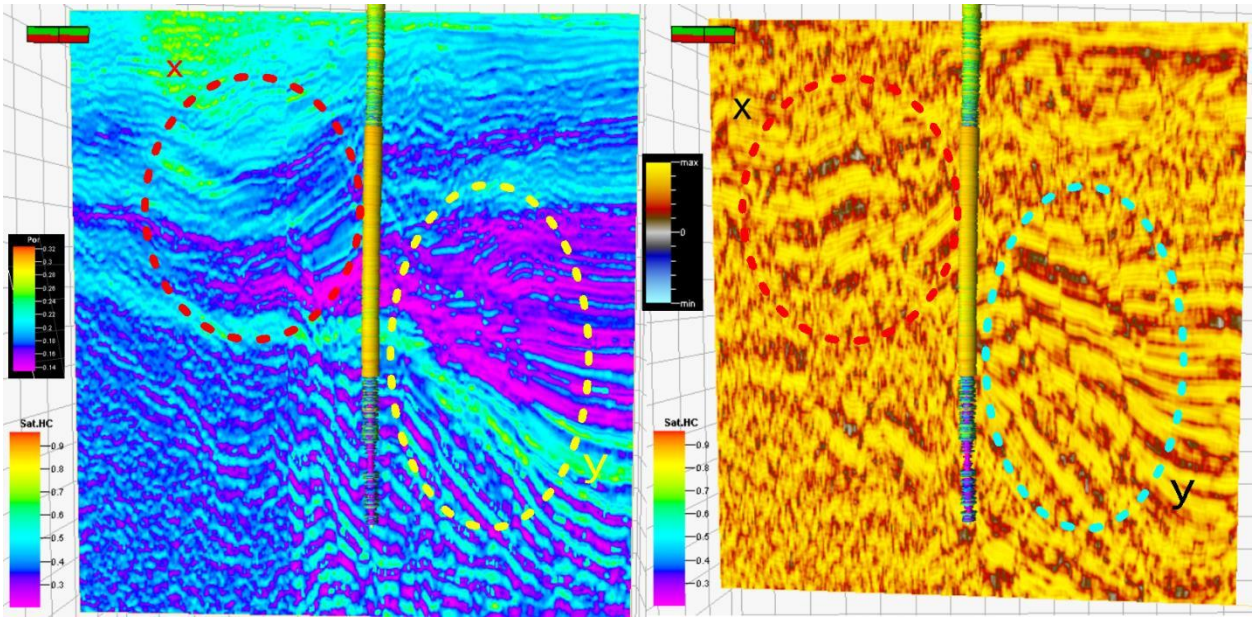

Figure 13 Porosity and rms amplitude lines with well U25. Saturation log property as overlay

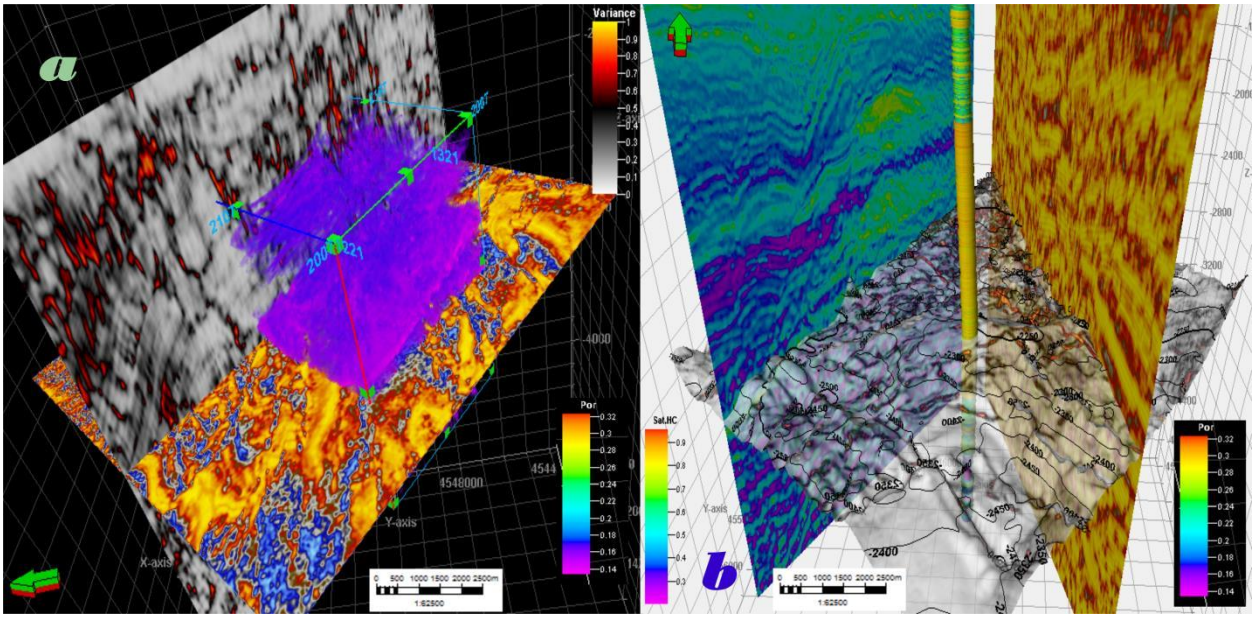

Figure 14 Porosity volume inserted within rms sand fairway surface and coherency line (a). Transparency embossed reservoir horizon with mirrored arbitrary line (b)

4. Prospect identification from petrophysical maps

To come to terms with the hydrocarbon occurrence and structural control on it, resistivity of the reservoir fluid was analyzed in relation to computed porosity and permeability. Vertical wells drilled cut through the hydrocarbon and non-hydrocarbon bearing zones. Average values of resistivity, porosity and permeability for 9 wells in the area (Figures 1 and 3) was computed and averaged for map generation of surfaces over structural traps. This was done in the vicinity of identified reservoir tops earlier interpreted on well logs. Variation in petrophysical values are seen literally across the area with the trap location having higher values. Consequently the highly porous and permeable portions are target for exploration.

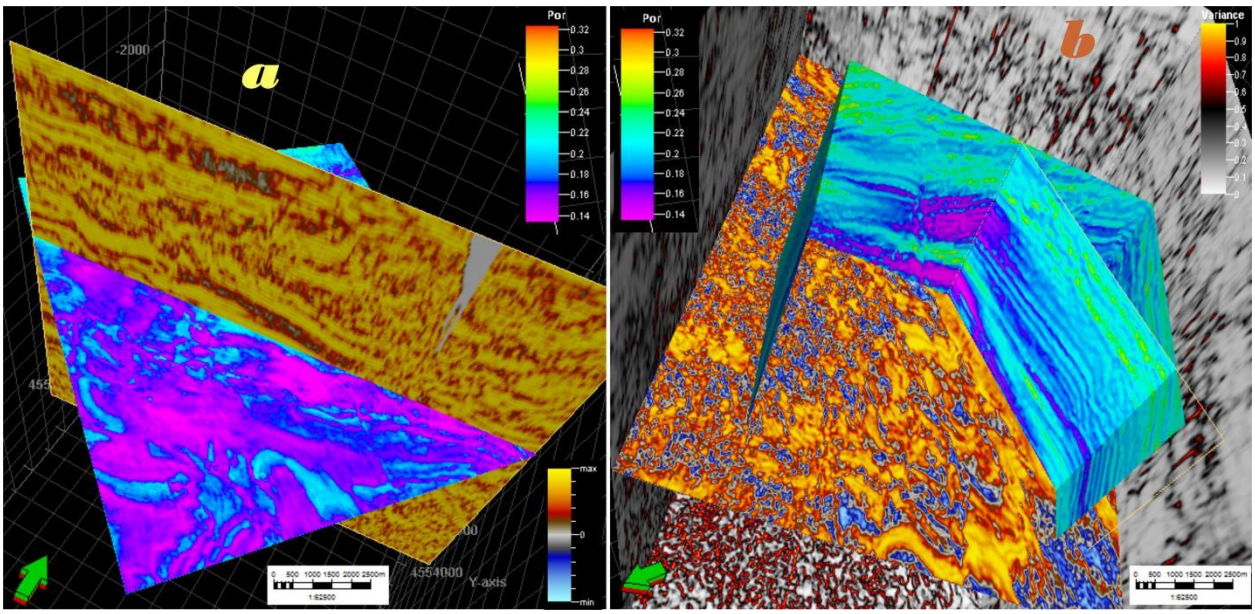

Figure 15 Continuous sand bodies with porosity property. This shows the potential of the sand deposit as hydrocarbon prolific in terms of porosity

These portions are controlled by the complex underlying basement structural architecture, faulting associations and pattern development in the field. This makes the upper strike slip set to run totally in different orientation with the buried major strike slip fault. This thereby causing stratigraphical control on the sediments deposited and makes it to adopt the present internal structural patterns. Because the deposits are progradationally emplaced on the basement and slope with series of synsedimentary and post-sedimentary extensive thrust fault patterns within the sag structure, fault echelon developed with parallel, sub-parallel and sigmoidal seismic patterns prevailing within the area. The hydrocarbon potential of this zone is further appreciated in the view of the overlaid visualizations done for porosity volume within the structural context. Figures 13 - 15 display this, portraying the variations of this rock property within the zone and across structural element.

5. Conclusions

The challenge of resolving lithological portions of the subsurface with high and proven hydrocarbon potential has been mitigated here by making use of seismic attributes and physicochemical parameters like porosity and hydrocarbon saturation. Volume attributes for understanding structural and stratigraphic patterns was been employed with emphasis on dispersed wave trace normalization through smoothing of seismic patterns and the enhancement of discontinuity and edge effects. Computations of structural attributes and some velocity attributes has assisted in understanding patterns seen on the generated stratigraphic attributes which had to be colour rendered on gray scale and RGB blending for pattern clarity.

Packets of sediments identified to be reservoir units were appraised with porosity and hydrocarbon saturation properties they are the prospects explored. This hydrocarbon bearing deposits fall within the most faulted zone having normal and reverse fault dominant. The faults appear in set and in some instances listric with anomalous patterns giving rise to horst and graben structures. Thus, prospective explorations targets inferred from the combination of these interpretation approach occurs on both the upthrown and downthrown blocks of the faults delineated and in interfingering sediments with porosity between 0.15 and 0.35. This zone has high hydrocarbon saturation and thus targeted for exploration.

Acknowledgements

The China Ministry of Science and Technology is appreciated for the equipment donation made available for this research under the CASTEP scheme. TWAS-CAS and IGGCAS is much appreciated for the research support and congenial environment.

References

[1] Barnes, A.E., 2003. Shaded relief seismic attribute. Geophysics 68, 1281-1285.

[2] Eissa, M. A., Pfeiffer J. and Ortega, H. A. P., 2009. Seismic petrophysical analysis for thin sandstone reservoirs in Colombia's Guajira Basin. The Leading Edge 6, 640-647.

[3] Hong, Z.M., and Yang, Z.J., 1984. The history of generation, development and evolution of the Tancheng-Lujiang fracture in Liaoning province. Geological Bulletin of China 10(3), 49-57 (in Chinese)

[4] James, H., Peloso, A., and Wang, J., 2002. Volume interpretation of multi-attribute 3D surveys. First Break, 20(3), 176-180.

[5] Li, S., Pang, X., Liu, K., Gao, X., Li, X., Chen, Z., and Liu, B., 2008. Formation mechanism of heavy oils in the Liaohe western depression, Bohai Gulf Basin. Science in China series D: Earth Science. 51(II), 156-169.

[6] Reijers, T. J. A., Petters, S. W. and Nwajide, C. S., 1997. The Niger Delta basin. In: Selley, R. C. (Eds.), African basins, Elsevier science, sedimentary basins of the world; 3, pp. 151–172.

[7] Reijers T.J.A., 2011. Stratigraphy and sedimentology of the Niger Delta. Geologos 17(3), 133–162

[8] Sierra, J., Campos, H., Bonilla, M., Paz, D., Marin, W., Cardinez, S., and Joseph, D., 2009. Seismic multiattribute integration for prospect generation in South Main Soldado Field, Gulf of Paria, Trinidad and Tobago. The Leading Edge 6, 684-689

[9] Surender S. M and Dean C., 2010. Multi Attribute Analysis - An effective visualization and interpretation technique. 8th Biennial International Conference and Exposition on Petroleum Geophysics ("Hyderabad 2010") P-171, 1-4.

[10] Tong, H., Fusheng, Y., Changbo, G., 2008. Characteristics and Evolution of strike – slip tectonics of the Liaohe Western Sag, Bohai Bay Basin. Petroleum Science 5, 223-229.

[11] Verm, R.W., and Hilterman, F.J., 1994. Lithologic color coded sections by AVO crossplot. 64th Annual International Meeting, SEG, Expanded Abstracts, 1092-1095.

[12 ao, Y.Z., and Fang, Z.J., 1981. "Tanlu Fault Colloquium" note. Seismology and Geology 3(2), 69-78.

[13] Yinhui, Z., Nansheng, Q., Yuan, Z., Cuicui, L., Jianping, L., Yonghua, G., and Xiongqi, P., 2011. Geothermal regime and hydrocarbon kitchen evolution of the offshore Bohai Bay Basin, North China. AAPG Bulletin, 95(5), 749–769.